Available online at www.sciencedirect.com

ScienceDirect

Geochimica et Cosmochimica Acta xxx (2013) xxx–xxx

Geochimica et Cosmochimica Acta

www.elsevier.com/locate/gca

Modeling the compositional evolution of recharging, evacuating, and fractionating (REFC) magma chambers: Implications for differentiation of arc magmas

Cin-Ty A. Lee [a,*], Tien Chang Lee [b], Chi-Tang Wu [a]

[a] Dept. of Earth Science, MS-126 Rice University, 6100 Main St., Houston, TX 77005, United States
[b] Dept. of Earth Sciences, University of California, Riverside, CA 92521, United States

Abstract

Equations are presented to describe the compositional evolution of magma chambers undergoing simultaneous recharge (R), evacuation (E), and fractional crystallization (FC). Constant mass magma chambers undergoing REFC will eventually approach a steady state composition due to the "buffering" effect of recharging magma. Steady state composition is attained after $\sim 3/(D\alpha_x + \alpha_e)$ overturns of the magma chamber, where D is the bulk solid/melt partition coefficient for the element of interest and α_x and α_e are the proportions of crystallization and eruption/evacuation relative to the recharge rate. Steady state composition is given by $C_{re}/(D\alpha_x + \alpha_e)$. For low evacuation rates, steady state concentration and the time to reach steady state scale inversely with D. Compatible ($D > 1$) elements reach steady state faster than incompatible ($D < 1$) elements. Thus, magma chambers undergoing REFC will eventually evolve towards high incompatible element enrichments for a given depletion in a compatible element compared to magma chambers undergoing pure fractional crystallization. For example, REFC magma chambers will evolve to high incompatible element concentrations for a given MgO content compared to fractional crystallization. Not accounting for REFC will lead to over-estimation of the incompatible element content of primary magmas. Furthermore, unlike fractional crystallization alone, REFC can efficiently fractionate highly incompatible element ratios because the fractionation effect scales with the ratio of bulk D's. By contrast, in pure fractional crystallization, ratios fractionate according to the arithmetic difference between the bulk D's.

The compositional impact of REFC should be most pronounced for magma chambers that are long-lived, have low rates of eruption/evacuation, and/or are characterized by high recharge rates relative to the mass of the magma chamber. The first two conditions are likely favored in deep crustal magma chambers where confining pressures are high and warm country rock decrease the cooling rates of magma chambers. By contrast, REFC should be less significant in shallow crustal magma chambers, which erupt and cool more efficiently due to lower confining pressures, colder country rock, and the cooling effects of hydrothermal systems. We thus speculate that the effects of REFC will be small in mid-ocean ridge settings and most pronounced in arc settings, particularly mature island arcs or continental arcs, where magma chambers >10 km depth are possible. This begs the question of whether high Fe^{3+}, H_2O and CO_2 (all of which can be treated as incompatible "elements") in arc basalts could be enhanced by REFC processes and thus not just reflect inheritance from the mantle source. We show that REFC can plausibly explain observed enrichments in Fe^{3+} and H_2O in arc melts without significant depletion in MgO. Because the difference between calc-alkaline and tholeiitic differentiation series is mostly likely due to higher water and oxygen fugacity in the former, it may be worth considering the effects of REFC. Thus, if REFC is more pronounced in deep crustal magma chambers, mature island arcs and continental arcs would tend towards calc-alkaline differentiation, whereas juvenile island arcs would be more tholeiitic.

To fully test the significance of REFC will require detailed analysis of other highly incompatible elements, but presently the relative differences in bulk D of such elements may not be constrained well enough. The equations presented here provide a framework for evaluating whether REFC should be considered when interpreting geochemical data in differentiated magmas.

* Corresponding author. Tel.: +1 713 348 5084.
E-mail address: ctlee@rice.edu (Cin-Ty A. Lee).

0016-7037/$ - see front matter
http://dx.doi.org/10.1016/j.gca.2013.08.009

Please cite this article in press as: Lee C. -T. A., et al. Modeling the compositional evolution of recharging, evacuating, and fractionating (REFC) magma chambers: Implications for differentiation of arc magmas. *Geochim. Cosmochim. Acta* (2013), http://dx.doi.org/10.1016/j.gca.2013.08.009

For completeness, we have also provided the more general equations for a magma chamber undergoing recharge (R), evacuation (E), crustal assimilation (A) and fractional crystallization (FC), e.g., REAFC, for constant mass, growing and dying magma chambers.

1. INTRODUCTION

This paper concerns the compositional evolution of magma chambers undergoing simultaneous recharge (R), eruption/evacuation (E), assimilation (A) and fractional crystallization (FC) Table 1. The basic concepts of magma differentiation via fractional crystallization are well understood and widely taught in introductory and advanced petrology/geochemistry courses (e.g., Gast, 1968; Shaw, 1970, 1979; Albarede, 1996; Zou, 2007). However, the concepts of magma evolution undergoing magmatic recharge are not commonly taught or shown in textbooks even though magma recharge was already suggested as an important process over thirty years ago (O'Hara, 1977; DePaolo, 1981; O'Hara and Matthews, 1981; Albarede, 1985; Hill et al., 1985; Hill, 1988; O'Neill and Jenner, 2012). The effects of recharge can be non-intuitive, resulting in much confusion. Thus, there is still debate over whether recharge plays an important role in controlling the compositions of differentiating magmas (Hofmann, 2012; O'Neill and Jenner, 2012). In fact, few petrologic studies explore the role of recharge (Chiaradia et al., 2011). The more simplistic process of fractional crystallization (FC) is generally assumed. Here, we develop basic equations for modeling magma chamber compositional evolution during simultaneous magma recharge, evacuation, assimilation, and fractional crystallization (REAFC). Our analyses ultimately build on the seminal works of (O'Hara, 1977; DePaolo, 1981; O'Hara and Matthews, 1981; Albarede, 1985; O'Neill and Jenner, 2012), and in some respect, we have merely reproduced or reconfirmed their analyses. What we have tried to do differently is to provide additional intuition in understanding the compositional effects of recharge. Our equations are also more comprehensive in that they allow the user to simultaneously explore the effects of recharge, evacuation/eruption, fractional crystallization and crustal assimilation (REAFC). We also make new predictions in the context of new observations. Ultimately, our motivation is to reinvigorate the debate over recharging magma chambers so that the community can evaluate whether recharge in crystallizing and erupting magma chambers is important.

2. FRACTIONAL CRYSTALLIZING MAGMA CHAMBER

For the purposes of this paper, we define a magma "chamber" as any pool of magma, regardless of size, that has stalled in the crust or lithospheric mantle (Fig. 1). We treat the "chamber" mathematically as a box. This definition includes kilometer-sized magma bodies in the mid to upper crust, such as those that feed stratovolcanoes or large rhyolitic eruptions (Fig. 1a). Also included would be magmatic sills in the deep oceanic or continental crust (Fig. 1b and c). Mathematically, dikes can be considered in the same way; the only difference from a magma chamber is that the ratio of eruption or evacuation to crystallization is high (Fig. 1d). In all cases, these magma bodies are situated in cold country rock and therefore will cool, resulting in crystallization, which in turn leads to crystal segregation. Without recharge or wallrock assimilation, crystal segregation results in a progressive decrease in the mass of the residual liquid and a change in its composition. Eventually, the magma chamber will die by freezing.

Without recharge, evacuation or crustal assimilation, the compositional evolution of the residual liquid can be modeled by continuous segregation of crystals, using the well-known Rayleigh fractional crystallization equation (Gast, 1968; Greenland, 1970; Shaw, 1970, 1979; Albarede, 1996):

$$\frac{C_L}{C_o} = F^{D-1} \tag{1a}$$

where C_o is the initial concentration of the element in the magma before crystallization, C_L is the concentration in the residual liquid, F is the mass fraction of residual liquid relative to original mass of magma, and D is a bulk partition coefficient describing the enrichment of an element in the crystallizing solids relative to the liquid, that is, $D \equiv C_s/C_L$, where C_s is the concentration in the crystallizing assemblage (e.g., the solids). For a multiphase crystallizing assemblage, bulk D is the weighted average of the partition coefficients D_i for each phase, $D = \sum X_i D_i$, where X_i is the weight fraction of each phase *in the crystallizing assemblage*. From the definition of D, it follows that the concentration of an element in the instantaneous crystallizing assemblage is

$$\frac{C_S}{C_o} = DF^{D-1} \tag{1b}$$

These equations are relatively straightforward to implement. If an element is incompatible in the crystallizing assemblage, that is, if $D < 1$, the element becomes progressively enriched in the residual liquid as crystallization progresses and F decreases. The maximum enrichment of an incompatible element in the residual liquid is $1/F$ when the element is perfectly incompatible, that is, $D \ll 1$. When an element is compatible in the crystallizing assemblage, that is, $D > 1$, the element is rapidly depleted from the residual liquid with progressive crystallization. In the next section, we add the effects of recharge and eruption/evacuation.

3. AN ANALYTICAL MODEL FOR MAGMA CHAMBERS UNDERGOING RECHARGE, EVACUATION AND FRACTIONAL CRYSTALLIZATION (REFC)

We now consider the effects of recharge and eruption/evacuation. Continuous or episodic replenishment of

Please cite this article in press as: Lee C. -T. A., et al. Modeling the compositional evolution of recharging, evacuating, and fractionating (REFC) magma chambers: Implications for differentiation of arc magmas. *Geochim. Cosmochim. Acta* (2013), http://dx.doi.org/10.1016/j.gca.2013.08.009

Table 1
List of symbols used in text.

FC	Fractional crystallization
AFC	Assimilation and fractional crystallization
REFC	Recharge, evacuation/eruption, and fractional crystallization
REAFC	Recharge, evacuation, assimilation and fractional crystallization
D	Solid/melt or crystal/melt partition coefficient
C_L	Concentration of an element in magma or liquid
C_o	Concentration of an element in initial magma or liquid
M_{ch}	Mass of magma chamber
dM_x	Change in magma chamber mass due to crystal segregation
dM_e	Change in magma chamber mass due to eruption/evacuation
dM_{re}	Change in magma chamber mass due to recharge
dM_{cc}	Change in magma chamber mass due to crustal assimilation
$\alpha_x \equiv dM_x/dM_{re}$	Proportion of crystallization relative to recharge rate
$\alpha_e \equiv dM_e/dM_{re}$	Proportion of evacuation relative to recharge rate
C_x	Concentration of an element in crystals
C_e	Concentration of an element in erupting/evacuating magma
C_{re}	Concentration of an element in the recharging magma
C_{cc}	Concentration of an element in the crust assimilant
C_{ch}	Concentration of an element in the magma chamber
C^o_{ch}	Initial concentration of an element in the magma chamber
$m_{ch} = C_{ch}M_{ch}$	Total mass of a given element in the magma chamber
$\alpha_i \equiv dM_i/dM_{re}$	Ratio of mass change due to a give process relative to recharge
ΔM_{re}	Total time-integrated mass of recharged magma
$\Delta\overline{M}_{re} \equiv \Delta M_{re}/M_{ch}$	Number of turnovers for a constant mass magma chamber
$\Delta\overline{M}^*_{re}$	Number of turnovers required for compositional steady state
C^∞_{ch}	Concentration of an element at steady state
$t_{res} = M_{ch}/(dM_{re}/dt)$	Residence time
$\phi_i \equiv dM_i/dM_{ch}$	Ratio of mass added or subtracted due to a particular process relative to the mass change of the magma chamber

magma chambers should be expected for long-lived magma chambers situated above a region undergoing relatively continuous magmatic fluxing, such as in subduction zones and mid-ocean ridges. Replenishment of the magma chamber by new batches of magma through feeder dikes will decrease cooling and crystallization rates, the extent of which depends on the ratio of magma recharge relative to magma chamber volume.

We also expect magma chambers to undergo varying amounts of evacuation, depending on the depth and stress state of the magma chamber. In the case of shallow level magma chambers, such evacuation might manifest in the form of eruptions. In the lower crust, liquids evacuated from the magma chamber could rise to form shallower magma chambers and so forth, leading to a series of sills or small magma pools through which all magmas must pass

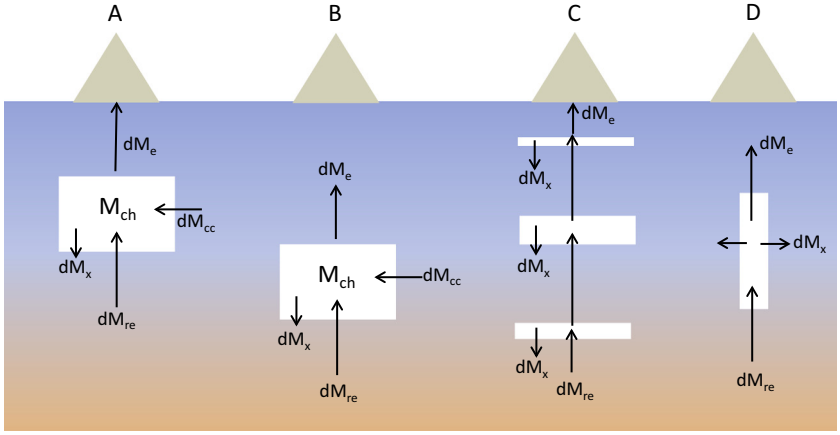

Fig. 1. Cartoon depicting different types of magma chambers. (A) and (B) show shallow and deep crustal magma chambers. (C) Magma differentiation occurs through a series of magma chambers. (D) Extreme case of a dike. While a dike is not a magma chamber, it can be modeled, geochemically, in a similar fashion. In a dike, one might expect eruption/evacuation to be high compared to crystallization along the conduit walls. In all figures, M_{ch} is the mass of the magma chamber, dM_e is the rate of eruption/evacuation, dM_{re} is the rate of recharge, dM_x is the rate of crystallization, and dM_{cc} is the rate of crustal assimilation/contamination. Arrows are schematic (length of arrows should not be taken literally).

Please cite this article in press as: Lee C. -T. A., et al. Modeling the compositional evolution of recharging, evacuating, and fractionating (REFC) magma chambers: Implications for differentiation of arc magmas. *Geochim. Cosmochim. Acta* (2013), http://dx.doi.org/10.1016/j.gca.2013.08.009

before they intrude into the upper crust or erupt (Fig. 1d). Intuitively, high eruption efficiency would shorten the residence time of magma in the chamber, reducing the effect of crystallization in modifying the composition of the magma chamber.

Recharge and evacuation effects have been explored previously. O'Hara (1977), O'Hara and Matthews (1981), Albarede (1985), and O'Neill and Jenner (2012) treated recharge as sequential, incremental processes. DePaolo (1981) developed analytical solutions for magma chambers undergoing continuous fractional crystallization and assimilation (AFC) by integrating the mass balance equations rather than by performing incremental calculations. He modified his equations to describe recharging magma chambers, although he did not include evacuation. When the increments of recharge and crystallization are small, the models converge to the integrated solutions, yielding relatively simple analytical solutions, as presented by DePaolo (1981). These analytical solutions are useful in that the physical meaning of the recharge-crystallization process are more easily understood. For this reason, we build on the approach of DePaolo (1981) in the following analysis.

The concentration of an element changes in a magma chamber undergoing continuous recharge, evacuation and fractional crystallization (REFC) can be modeled as follows. For a more general case in which crustal assimilation is considered (e.g., REAFC), see Appendix A1. Mass balance requires that the change in the total amount of an element in the magma chamber is equal to the sum of the mass inputs (recharge) and outputs (fraction crystallization and evacuation) of the element (Fig. 1):

$$dm_{ch} = d(C_{ch}M_{ch}) = -C_x dM_x - C_e dM_e + C_{re} dM_{re} \tag{2}$$

where lowercase m denotes the mass of the element (m_{ch} is the mass of the element in the magma chamber) and uppercase M denotes the total mass of the magma chamber (M_{ch}), crystals (M_x), evacuated magma (M_e) and recharging magma (M_{re}) and C_{ch}, C_x, C_e and C_{re} are the concentrations by weight of the element in the magma chamber and in the crystallizing, evacuating, and recharging fractions. The differentials denote an increment of mass change in a given time increment. C_x is related to the concentration in the residual liquid in the magma chamber C_{ch} by an equilibrium partition coefficient D between crystals and melt, $C_x \equiv DC_{ch}$. The evacuated/erupted magma should have the same composition as that in the magma chamber, hence $C_e = C_{ch}$.

For simplicity, we will assume the case in which the mass of the magma chamber M_{ch} is at steady state, that is,

$$dM_x + dM_e = dM_{re} \tag{3}$$

For the more general case of growing or decreasing magma chamber, the reader should refer to Appendix A2. Eq. (3) can be divided on both sides by dM_{re}, resulting in

$$\alpha_x + \alpha_e = 1 \tag{4}$$

where

$$\alpha_x \equiv dM_x/dM_{re} \tag{5a}$$

$$\alpha_e \equiv dM_e/dM_{re} \tag{5b}$$

and refer to the ratios of crystallization and evacuation to recharge rates, respectively. Substituting Eqs. (5a) and (5b) into Eq. (2) yields

$$M_{ch}dC_{ch} = (-D\alpha_x C_{ch} - \alpha_e C_{ch} + C_{re})dM_{re} \tag{6}$$

Moving the quantity in parentheses into the denominator on the left hand side and using the relation $dC/C = d(\ln C)$, Eq. (6) can be integrated from $\Delta M_{re} = 0$, where $C_{ch} = C^o_{ch}$, to ΔM_{re}. This yields an expression for REFC

$$\frac{C_{ch}}{C^o_{ch}} = \frac{C_{re}/C^o_{ch}}{D\alpha_x + \alpha_e} - \left[\frac{C_{re}/C^o_{ch}}{D\alpha_x + \alpha_e} - 1\right] \exp\left[-\Delta\overline{M}_{re}(D\alpha_x + \alpha_e)\right] \tag{7a}$$

where C^o_{ch} is the initial concentration in the magma chamber and $\Delta\overline{M}_{re}$ is defined as

$$\Delta\overline{M}_{re} \equiv \Delta M_{re}/M_{ch} \tag{8}$$

and represents the *integrated* amount of magma $\Delta M_{re} = \int dM_{re}$ recharged *relative* to the magma chamber mass (for a constant mass magma chamber ΔM_{re} is equal to the total amount of crystallized products). In other words, $\Delta\overline{M}_{re}$ represents the number of times the magma chamber has turned over. Eq. (7a) can be simplified for the special case in which the recharging magma is the same as the parental magma, e.g. $C_{re} = C^o_{ch}$, hence

$$\frac{C_{ch}}{C^o_{ch}} = \frac{1}{D\alpha_x + \alpha_e} - \left[\frac{1}{D\alpha_x + \alpha_e} - 1\right] \exp\left[-\Delta\overline{M}_{re}(D\alpha_x + \alpha_e)\right] \tag{7b}$$

The composition of the instantaneous cumulate C_x is given by DC_{ch}. Note that if $\alpha_e = 0$, that is, evacuation or eruption is zero, Eq. (7b) is very similar to Eq. (23) in Section 2.3 of DePaolo (1981). We have also expressed the equation in terms of the number of overturns or accumulated recharge events, whereas DePaolo used the integrated cumulate mass as a progress variable. This difference in expression is important when evacuation is non-zero.

The key features of a constant mass magma chamber undergoing simultaneous replenishment, crystallization and evacuation is that the composition of the magma chamber will initially be that of the parental magma, but as the chamber crystallizes, erupts and recharges, it will evolve to a *compositional* steady state due to the buffering effect of continuous recharge (Fig. 2). For an analytical solution, we assume that the composition of the recharging magma is constant. For the more general case in which the recharging magma changes composition, numerical approaches are required and the reader is referred to our Excel program in Appendix A3. The number of overturns $\Delta\overline{M}_{re}$ needed to reach compositional steady state will scale with the e-fold time (e.g., $e = 2.718$), such that the number of overturns needed to reach within 10% of steady state is ~3 times the e-fold time, that is,

$$\Delta\overline{M}^*_{re} \sim \frac{3}{D\alpha_x + \alpha_e} \tag{9}$$

Please cite this article in press as: Lee C. -T. A., et al. Modeling the compositional evolution of recharging, evacuating, and fractionating (REFC) magma chambers: Implications for differentiation of arc magmas. *Geochim. Cosmochim. Acta* (2013), http://dx.doi.org/10.1016/j.gca.2013.08.009

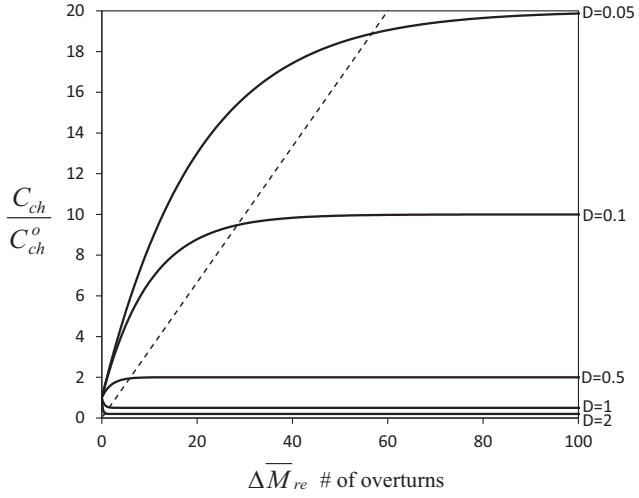

Fig. 2. Concentration enrichment/depletion factor (e.g., concentration relative to initial value or recharging magma, C_{ch}/C^o_{ch}) in a constant mass magma chamber as a function of the number of overturns $\Delta\overline{M}_{re}$ for elements with different bulk partition coefficients D ($D > 1$ is compatible, $D < 1$ is incompatible). Dashed line indicates number of overturns required to reach steady state. Eruption/evacuation and crustal assimilation are assumed to be zero.

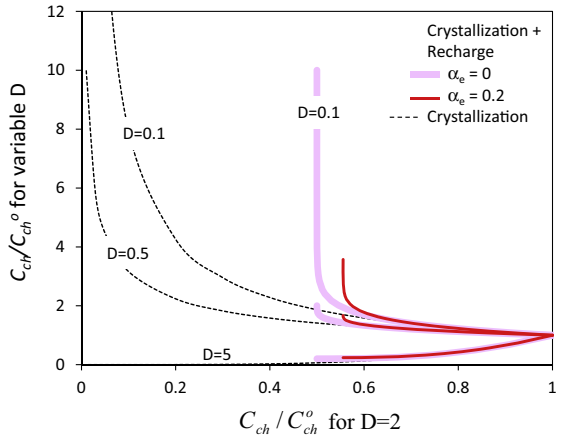

Fig. 3. Concentration enrichment/depletion factor (C_{ch}/C^o_{ch}) of elements with variable partitioning behavior ($D = 0.1$, 0.5, and 5) in a constant mass magma chamber as a function of the concentration of a compatible element (x-axis) with $D = 2$ during differentiation. "One can view the x-axis as analogous to MgO and the y-axis to an incompatible element, such as Ce (D=0.1)." Dashed lines correspond to pure fractional crystallization (FC), in which recharge, evacuation and assimilation are zero. Thick pink lines correspond to a constant mass magma chamber undergoing recharge and crystallization (RFC), but no evacuation ($\alpha_e = 0$). Thin red lines show a recharging, evacuating and crystallizing (REFC) magma chamber for the case in which 20% of the mass output from the magma chamber (evacuation + crystallization) occurs through eruption/evacuation ($\alpha_e = 0.2$) and remaining 80% by crystallization. Note that in recharging systems, incompatible elements rise to higher values for a given concentration of a compatible element due to the more soluble nature (and hence longer residence time) of incompatible elements in the magma. Increasing evacuation efficiency causes the steady-state composition of the magma to converge towards the parental recharging magma. (For interpretation of the references to colour in this figure legend, the reader is referred to the web version of this article.)

where the steady state composition is given by

$$C^{\infty}_{ch} = \frac{C_{re}}{D\alpha_x + \alpha_e} \tag{10}$$

For the case in which evacuation is zero, $\alpha_e = 0$, Eqs. (9) and (10) imply that both the number of overturns needed to reach compositional steady state, as well as the composition at steady state, scale inversely with D. In other words, incompatible elements ($D < 1$) require more overturns than compatible elements ($D > 1$) to reach steady state. When eruption/evacuation of the magma chamber is not zero, e.g., $\alpha_e > 0$, the number of overturns required to reach steady state (Eq. (9)) decreases and the steady state composition of the magma chamber approaches that of the recharging magma. In the extreme case in which all magma erupts and no crystallization occurs ($\alpha_e = 1$ and $\alpha_x = 0$), the composition of the erupting magma, the magma chamber, and the recharging magma converge as expected.

It is straightforward to relate the number of overturns to time if the recharge rate $\dot{M}_{re} = dM_{re}/dt$ is known. For a constant magma chamber mass, the number of overturns, $\Delta\overline{M}_{re}$, is related to the residence time of the magma in the chamber as follows. The average time a parcel of magma resides in the magma chamber (e.g., the residence time) is given by

$$t_{res} = M_{ch}/\dot{M}_{re} \tag{11}$$

where $\dot{M}_{re} = dM_{re}/dt$ is the rate of magma replenishment. The total time elapsed for $\Delta\overline{M}_{re}$ overturns is then $t_{res}\Delta\overline{M}_{re}$.

The above concepts can be understood further if we consider specific examples. Let's consider the magmatic evolution of a trace element, such as the light rare Earth element Ce, and a major element, such as Mg (denoted as MgO by convention) (Fig. 3). Let us also begin with a primitive basalt as the parental magma. In such a case, early fractionation is dominated by olivine crystallization, so Ce is highly incompatible and MgO is compatible in the crystallizing

assemblage. Let's assume constant partition coefficients of 0.1 for Ce and 2 for MgO (O'Neill and Jenner, 2012). In reality, partition coefficients will change with decreasing temperature and changing magma composition, but this simplification captures the first order behavior of the magmatic system (for the more general case of changing partition coefficients, the reader should refer to the numerical software provided in the Appendix A3).

In the pure fractional crystallization (FC) case (no evacuation and no recharge), Ce increases and MgO decreases indefinitely so no steady state composition is ever reached (Fig. 3). However, extreme enrichment in Ce occurs only after significant fractional crystallization (e.g., small residual melt fraction F), which corresponds to extreme depletion in MgO. For example, it can be seen in Fig. 3 that enrichment of Ce by FC is significant only after MgO has decreased by a factor of 10. By contrast, for a recharging-crystallizing magma chamber, e.g, REFC (we consider for simplicity the case in which evacuation is zero), significant Ce enrichment occurs at intermediate MgO contents, e.g., when MgO has decreased by only a factor of 2, because MgO reaches a steady state value of one-half that of the parental magma after only ~1 overturn, whereas Ce reaches a steady state value of 10 times that of the parental magma after ~10 overturns based on Eqs. (9) and (10). Thus, for a given compatible element concentration, such as MgO, incompatible elements will be higher in a recharging-crystallizing magma than in a system undergoing pure fractional crystallization. Because of the rapid attainment of steady state for a compatible element compared to that of an incompatible element, one would also predict recharging-crystallizing magma chambers to have highly variable incompatible element concentrations but more uniform compatible element concentrations. If evacuation is considered, steady state is attained earlier and the steady state concentrations approach that of the parental magma for both compatible and incompatible elements.

4. A PEDAGOGICAL ANALOGY WITH THE OCEAN

One way to better understand the above concepts is to consider the ocean as analogous to a magma chamber. By mass, the ocean is at steady state, balanced by freshwater input (riverine and rain recharge) and evaporative outputs. Let us consider two elements, Na and Fe. Na is highly soluble in seawater (analogous to being incompatible in precipitating phases from seawater or in the evaporative flux) and Fe is insoluble in seawater because it precipitates as Fe–Mn oxyhydroxides once it oxidizes (analogous to a compatible element). The Na concentration in seawater (1.08×10^7 μg/L) is ~2000 times higher than that in riverine freshwater (6.0×10^3 μg/L), whereas the Fe concentration of seawater (5.59×10^{-2} μg/L) is ~700 times *less* than riverine freshwater (4×10^1 μg/L). These seawater concentrations can be explained in the context of the above discussions. Steady state concentration scales inversely with partition coefficient (Eq. (10)) or, in this case, positively with solubility, which is effectively the inverse of the partition coefficient. Thus, it is obvious that soluble Na will become highly concentrated in seawater, whereas insoluble Fe becomes depleted. Analogous to a recharging, crystallizing and erupting magma chamber, recharge of the ocean by freshwater riverine input keeps the oceans from becoming excessively saline by evaporation. Similarly, riverine input keeps the oceans from being completely depleted of Fe by precipitation of Fe oxyhydroxides.

At compositional steady state, we can also define the average residence time of Na and Fe in the oceans. Eq. (9) shows that the residence time should scale inversely with the partition coefficient (or positively with solubility in seawater). The residence time of an element in the ocean is

$$t_{res} = \frac{m_{oc}}{dm_{re}/dt} = \frac{C_{oc}M_{oc}}{C_{re}(dM_{re}/dt)} \tag{12}$$

where m_{oc} is the mass of the element in the ocean, dm_{re}/dt is the mass inflow of the element into the ocean via rivers, C_{oc} is the concentration in the ocean, M_{oc} is the mass of water in the ocean (1.4×10^{21} kg), C_{re} is the concentration river waters, and dM_{re}/dt is riverine flow rate (3.6×10^{16} kg/y). Thus, the residence times of Na and Fe in the oceans are ~70 My and 50 y, respectively. These residence times are equivalent to the relaxation time of the ocean system to perturbations (Lasaga, 1998). A perturbation in the inputs of Na would take much longer to return to steady state than a perturbation in Fe inputs. Of course, because of the high concentration of Na in the ocean, the ocean will largely be insensitive to perturbations in Na unless the perturbation is extremely large.

5. IMPLICATIONS

5.1. Comparison with fractional crystallization

Magma differentiation is commonly assumed to be controlled by fractional crystallization, so that if the effects of fractional crystallization can be properly corrected for, the composition of the parental magma can be obtained (Weaver and Langmuir, 1990; Collier and Kelemen, 2010; Till et al., 2012). This correction, albeit highly simplified, has become common practice, and is motivated by the desire to infer the parental magma composition to estimate pressure, temperature and composition of the magma source (Putirka, 2005; Herzberg et al., 2007; Putirka et al., 2007; Herzberg and Asimow, 2008; Lee et al., 2009). However, if magma chambers are continually recharged, applying a fractional crystallization correction alone would severely over-estimate the primary magma concentrations for an incompatible element. For example, at MgO/MgO_i of 0.5, fractional crystallization enriches Ce by only 2 times, whereas recharge-crystallization enriches the magma Ce anywhere from 3 to 100 times (Fig. 3). Failure to account for recharge-crystallization would give the impression that the magma derived from an enriched parental magma, even though its enriched signature is an effect of REFC. Recharging magma chambers tend to erase the history of the primary magma.

Another difference between FC and REFC is the effect on trace element ratios. It is generally assumed that magmatic differentiation cannot change ratios between highly incompatible elements so element ratios, such as Ce/H_2O,

Please cite this article in press as: Lee C. -T. A., et al. Modeling the compositional evolution of recharging, evacuating, and fractionating (REFC) magma chambers: Implications for differentiation of arc magmas. *Geochim. Cosmochim. Acta* (2013), http://dx.doi.org/10.1016/j.gca.2013.08.009

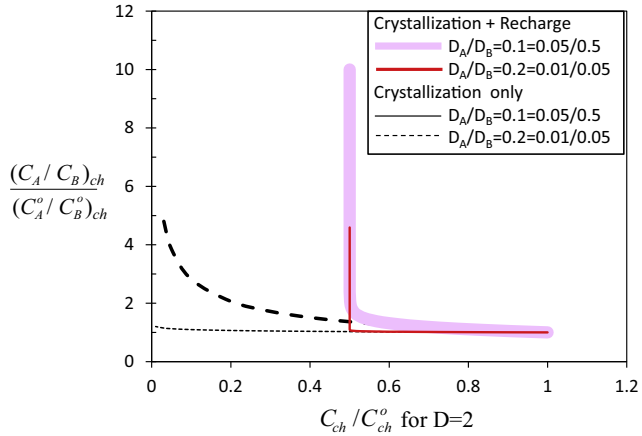

Fig. 4. Same as in Fig. 3 except that the *y*-axis shows the ratio of two incompatible elements in the magma chamber normalized to the same quantity in the recharging magma. Dashed lines correspond to the case in which the elemental ratio is controlled by pure fractional crystallization. Such a scenario does not significantly fractionate the elemental ratio as discussed in the text. Pink and red lines correspond to a constant mass magma chamber balanced by recharge and crystallization. Thick pink line corresponds to the case in which the ratio of the incompatible element partition coefficients is large (0.5). The thin red line depicts an elemental pair that might also be interesting. (For interpretation of the references to colour in this figure legend, the reader is referred to the web version of this article.)

Nb/La, Ba/Nb, Nb/CO_2, and Ce/Pb, remain constant during differentiation and therefore reflect the composition of the primary magma. This assumption is based on the simple concept of fractional crystallization as described in Eq. (1a). For the ratio of elements A to B, the equivalent of Eq. (1a) for FC is

$$\frac{(C_A/C_B)}{(C^o_A/C^o_B)} = F^{D_A-D_B} \quad \text{for FC} \tag{13}$$

Elemental fractionation during FC scales with melt fraction to the power of the *arithmetic difference* between the two partition coefficients. Because $D < 0.1$ for a highly incompatible element, the difference between the partition coefficients of two incompatible elements is always $\ll 0.1$, even if the two partition coefficients are not identical. Another way to present this concept is that elements that are highly soluble in the melt will therefore behave conservatively in the melt so that their relative proportions do not change. This is why incompatible element ratios do not fractionate in the magma during FC (Fig. 4).

However, for simultaneous recharge-crystallization (REFC), incompatible element ratios can potentially fractionate significantly if their D's, while small, are not exactly identical. To illustrate, we consider elemental ratios at steady state, that is, after a large number of overturns. From Eq. (7b), the elemental fractionation at steady state composition during REFC is given by

$$\frac{(C_A/C_B)}{(C^o_A/C^o_B)} = \frac{D_B\alpha_x + \alpha_e}{D_A\alpha_x + \alpha_e} \quad \text{for REFC} \tag{14}$$

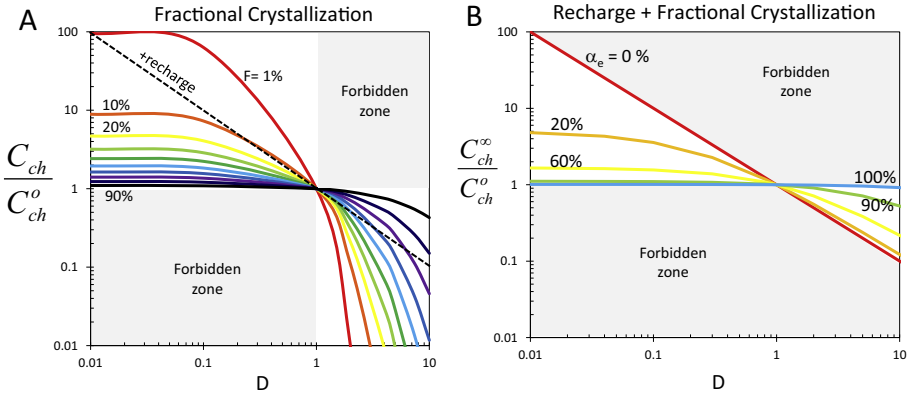

Fig. 5. y-Axis shows relative enrichments or depletions in elements C_{ch}/C^o_{ch}) as a function of their partition coefficients D for fractional crystallization (A) and magma chambers undergoing recharge, fractional crystallization and variable amounts of evacuation α_e (B). In fractional crystallization (A), the enrichment/depletion scales with the amount of residual magma F, as shown by the different curves for each F. Dashed line in (A) represents the steady state relationship for recharging magma chamber with zero evacuation. Shaded area in (A) represents zone in which enrichments or depletions are forbidden. In the case of recharging and crystallizing magma chambers (B), enrichment/depletion scales log-linearly with D. If evacuation occurs, the sense of the concentration-D relationship becomes more similar to that of fractional crystallization.

Please cite this article in press as: Lee C. -T. A., et al. Modeling the compositional evolution of recharging, evacuating, and fractionating (REFC) magma chambers: Implications for differentiation of arc magmas. *Geochim. Cosmochim. Acta* (2013), http://dx.doi.org/10.1016/j.gca.2013.08.009

which means that the element ratio scales inversely with the *ratio* of the partition coefficients (if α_e is ~1, there is no fractionation), not with the arithmetic difference. For example, if $D_A = 0.03$ and $D_B = 0.06$, C_A/C_B can be fractionated by a factor of 2 after ~33 overturns in a REFC magma chamber. In contrast, in the case of FC, elemental ratio fractionation is negligible (Fig. 4). Even at 99% crystallization, C_A/C_B increases by only 1.14 times during FC because it is the difference (0.03) between partition coefficients that matters; in fact, to increase the ratio by a factor of 2 by FC would require crystallization to progress until only 10^{-8}% liquid remains, which is volumetrically insignificant to be of any importance. Thus, the only way that the ratio of two elements, even if incompatible, can remain constant in a recharging-crystallizing magma chamber is if their partition coefficients are nearly identical or if the evacuation to crystallization ratio is large. In other words, magma chambers that efficiently erupt/evacuate will show little elemental fractionation, but long-lived magma chambers that are largely balanced by recharge and crystallization (e.g., no evacuation), are likely to show large fractionations unless the partition coefficients are identical, which seems, in general, unlikely. Given that the uncertainties for highly incompatible element partition coefficients can be very large, it is not clear if the partitioning of elements in canonical ratios, such as Ce/H_2O, Nb/La, Ba/Nb, Nb/CO_2, Ce/Pb are truly identical.

One additional difference between fractional crystallization and recharge is in how enrichment/depletion varies with D. By inspecting Eq. (1a) and (1b), it can be seen that the logarithm of the normalized magma concentration is negative linearly correlated with D, with the slope corresponding to the logarithm of F. For a constant mass recharging magma chamber, the logarithm of the normalized magma concentration correlates negatively with the logarithm of D at steady state if evacuation is zero. If there is evacuation, the correlation weakens. These differences can be readily seen on a plot of $\log(C_{ch}/C_{ch}^o)$ versus $\log(D)$ and are in exact agreement with O'Hara and Matthews (1981) (Fig. 5).

5.2. Conditions that favor recharge

As discussed above, significant enrichment in an incompatible element requires numerous chamber overturns. Because the residence time of magma in a chamber is $t_{res} = M_{ch}/(dM_{re}/dt)$, multiple overturns are favored when: (1) magma chambers are small for a given magma supply rate, (2) magma supply rate is high for a given magma chamber size, and (3) when the lifespan of a magma chamber is greater than the residence or overturn time of magma in the chamber. Another requirement for significant enrichment in an incompatible element is that the eruption/evacuation rate is small compared to the crystallization rate, that is, $\alpha_e/\alpha_x < 1$. Based on these criteria, we can make some qualitative generalizations about the types of environments in which the geochemical influence of magma recharge is significant.

For example, diking is more efficient under tension than under compression (Rubin, 1995), so evacuation efficiency should be high ($\alpha_e/\alpha_x > 1$) in extensional environments. All other quantities, such as magma supply rate and chamber size staying the same, magma chambers in extensional environments might be expected to be more primitive and show less divergence in composition from simple fractional crystallization trends than magmas in compressional environments. We can also consider differences between deep (>5 km) versus shallow (<5 km) magma chambers. Because the deep crust is warmer than the shallow crust, we would expect shallow magma chambers to cool and "die" more quickly than deep crustal magma chambers. Shallow crustal magma chambers might also be influenced by hydrothermal circulation, hastening their cooling and death (Norton, 1984). We might also expect diking in the deep crust to be more difficult than in the shallow crust due to the greater lithostatic pressure experienced by deep magma chambers, suggesting that evacuation efficiency in deep magma chambers would be less efficient than in shallow magma chambers. Numerical models of magma chamber dynamics indeed suggest that deep crustal magma chambers are less likely to erupt than shallow magma chambers for a given recharge rate (Karlstrom et al., 2010). Finally, deep crustal magma chambers might be favored in compressional environments. Indeed, inversion studies of InSAR-determined crustal deformation suggest that deep crustal magma chambers are more commonly found in compressional arcs, particularly continental arcs, than in island arcs (Chaussard and Amelung, 2012). For example, extensional arcs have magma chambers between <1 and 7 km in depth (Chaussard and Amelung, 2012). By contrast, magma chambers beneath much of the Andes, which are undergoing compression or transpression, have been inferred to be at depths between 5 and 10 km. The presence of cumulates from >20 km depth beneath continental arcs suggests even deeper magma chambers are possible in these environments (DeBari and Sleep, 1991; Mukhopadhyay and Manton, 1994; Ducea and Saleeby, 1996, 1998; Ducea, 2002; Lee et al., 2006, 2007, 2012; Jagoutz et al., 2007; Jagoutz, 2010; Lee, 2013). Simultaneous recharge and fractional crystallization processes have been invoked to explain the geochemistry of the plutons and deep-seated cumulates in the Sierra Nevada batholith, California (Lee et al., 2006).

As for magma chamber size, it is not clear how this property might vary with different tectonic environments or depth. There are reasons to believe that deep crustal magma chambers might be larger. Because deep crustal magma chambers have lower evacuation rates (Karlstrom et al., 2010) and the wall rock at depth is hot and hence weak, recharging chambers could grow by deforming the wallrock (Jellinek and DePaolo, 2003). It has also been suggested that warm temperatures of the deep crust make the wallrock easier to assimilate into the magma chamber, further facilitating chamber growth (Karlstrom et al., 2010). Nevertheless, upper crustal magma chambers might also be allowed to grow through erosional unroofing of the Earth's surface. Furthermore, it is also possible that magmas in the lower crust are distributed as a series of thin (200 m) sills (Annen et al., 2006) or small dikes (Dufek and Bergantz, 2005) rather than as large magma chambers. If distributed as thin sills, the ratio of recharge rate to magma chamber size might be predicted to be large.

Please cite this article in press as: Lee C. -T. A., et al. Modeling the compositional evolution of recharging, evacuating, and fractionating (REFC) magma chambers: Implications for differentiation of arc magmas. *Geochim. Cosmochim. Acta* (2013), http://dx.doi.org/10.1016/j.gca.2013.08.009

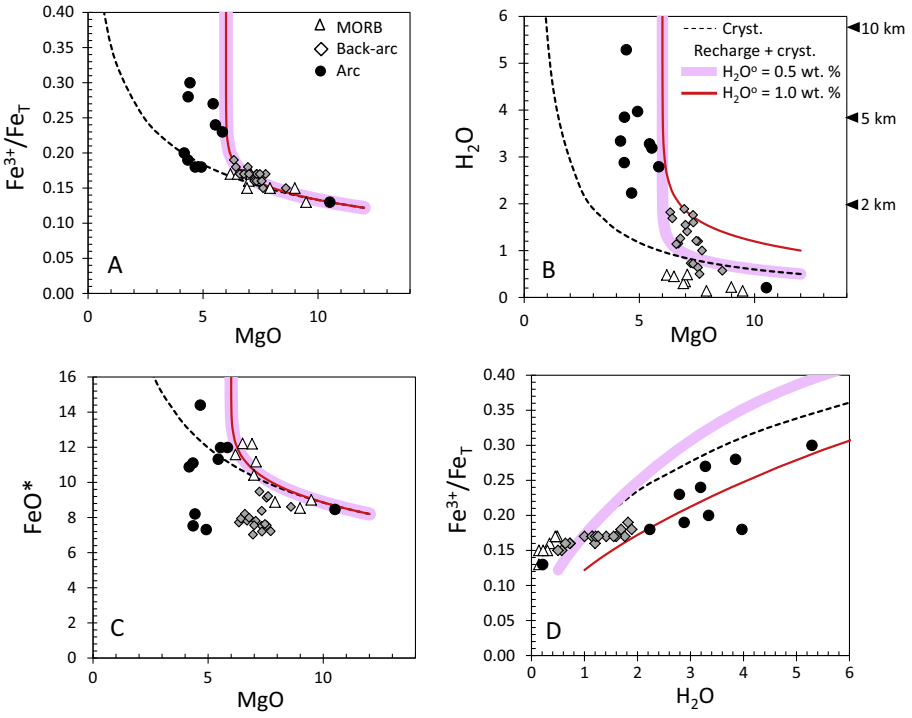

Fig. 6. Effects of recharge and fractional crystallization in a constant mass magma chamber without evacuation on Fe^{3+}/Fe_T and H_2O. *D* for Fe^{3+} is 0.1, Fe^{2+} is 0.8, H_2O is 0, and MgO is 2. (A) Atomic Fe^{3+}/Fe_T versus MgO (wt.%), where Fe_T corresponds to total Fe ($Fe^{2+} + Fe^{3+}$). (B) H_2O (wt.%) versus MgO (wt.%). (C) FeO* (Fe^{2+} and Fe^{3+} as FeO) in wt.% versus MgO (wt.%). (D) Fe^{3+}/Fe_T atomic ratio versus H_2O in wt.%. Dashed lines correspond to the pure fractional crystallization case. Thick pink line and thin red line correspond to recharging and crystallizing magma chamber. Thick pink line corresponds to a recharging and parental magma of 0.5 wt.% H_2O and thin red line is for a recharging and parental magma of 1.0 wt.% H_2O. Symbols represent melt inclusion compositions (Kelley and Cottrell, 2009). In B, right-hand axis shows the depth at which basaltic magmas of different initial water contents would saturate in a free fluid phase (Witham et al., 2012; Plank et al., 2013). (For interpretation of the references to colour in this figure legend, the reader is referred to the web version of this article.)

In summary, deep crustal magma chambers in compressional environments should have longer lifespans and exhibit less efficient eruption/evacuation rates than shallow magma chambers in extensional environments. Thus, numerous overturns as well as more pronounced compositional deviation from fractional crystallization trends would be expected in deep magma chambers compared to shallow ones. This leads us to speculate that recharge effects might be more important in arcs than at mid-ocean ridges because magmas must traverse thicker crust and lithosphere in arcs. In other words, if recharge is important in mid-ocean ridge environments, as recently suggested (O'Neill and Jenner, 2012), it must be even more important in arcs. We might further expect recharge to be more pronounced in continental arcs than island arcs because the former are thicker and more likely to be in compression than island arcs, which are typically extensional (Uyeda and Kanamori, 1979; Uyeda, 1982).

The potential implications for arc magmas are as follows. The volume flux of arc magmas passing through the Moho is ~2.4 $km^3/km^2/My$, estimated by dividing an approximate magma volume flow per length of arc of ~120 $km^3/km/My$ (Jicha et al., 2006) by the width of an active arc (~50 km). Assuming that lower crustal magma chambers occur as sills spread over the width of the active arc and that sill thicknesses are ~200 m (Annen et al., 2006), the magma body will go through one overturn in ~0.08 My. Thus, in 2 My, a 200 m sill would undergo ~24 overturns, enough to cause a >24-fold enrichment in Ce, but only a factor of two depletion in MgO. It is not clear how long magma chambers live in the lower crust, but if there is a steady supply of basaltic magma, magma chambers could persist for several million years (Annen et al., 2006; Gelman et al., 2013). In the upper crust, magma chambers would be expected to chill faster, decreasing the influence of magma recharge.

5.3. Implications for incompatible, volatile and redox-sensitive elements in arc magmas and the origin of calc-alkaline differentiation series

Arc lavas are commonly enriched in highly incompatible elements/species, such as CO_2, H_2O, large ion lithophile elements (Cs, Rb, Ba), and the light rare Earths (Gill, 1981; Leeman, 1996; Zimmer and Plank, 2006; Kelley and Cottrell, 2009) (Fig. 6). Arc lavas are also enriched in Fe^{3+} and are thus oxidized relative to mid-ocean ridge basalts (Carmichael, 1991; Kelley and Cottrell, 2009) (Fig. 6). These enrichments are generally thought to be primarily sourced in the mantle, presumably a mantle wedge that has been metasomatized by fluids derived from dehydration of subducting slabs (Gill, 1981; Leeman, 1996; Kelley and

Cottrell, 2009). While the mantle source of arc magmas is undoubtedly more enriched in incompatibles and water than mid-ocean ridge mantle, the question is what fraction of the enriched character of arc magmas can be explained by magma chambers undergoing REFC?

Assuming a bulk D_{Mg} of ~2 (O'Neill and Jenner, 2012), the steady state MgO content of the magma chamber will be 0.5 less than that of the primary magma, that is, if the primary magma has a MgO content of ~12 wt.% MgO, that of the magma chamber will be buffered at ~6 wt.% MgO. Incompatible elements/species, such as H_2O, would become highly enriched, depending on the exact number of overturns. We would also expect the oxidation state of Fe (e.g., molar Fe^{3+}/Fe_T ratio, where Fe_T is total the sum of Fe^{2+} and Fe^{3+}) to initially increase with progressive overturns because Fe^{3+} is incompatible in silicate minerals; once Fe^{3+} reaches magnetite saturation, Fe^{3+} will then decrease in the residual magma. If the oxygen fugacity of the magma is not externally buffered, then this increase in Fe^{3+}/Fe_T will increase the oxygen fugacity of the magma. The relative rate at which Fe^{3+}/Fe_T increases may be slightly lower than that of H_2O or CO_2 because small amounts of Fe^{3+} partition into clinopyroxene and spinel while Fe^{2+} is moderately incompatible in silicate minerals (Canil et al., 1994). In any case, because it would take numerous overturns (>100 for a D of 0.01) for H_2O, CO_2 and Fe^{3+} to reach their steady state concentrations, one would expect *increases* in H_2O, CO_2 and Fe^{3+}/Fe_T to be highly correlated with each other but show no correlation with compatible elements, such as Mg, which reaches its steady state value after less than one overturn. Thus, one outcome of simultaneous crystallization and recharge is the generation of a second stage "parental" magma with high H_2O, CO_2 and Fe^{3+} concentrations for a given MgO content (Fig. 6), and from this second stage basalt derives all subsequent differentiated magmas.

Enrichment in H_2O, CO_2 and Fe^{3+} will terminate if fluid or magnetite saturation is achieved. In the case of H_2O and CO_2, saturation results in vapor exsolution, which may, in turn, trigger evacuation or eruption due to the buildup of overpressure. The dissolved water content at the point of eruption then defines the pressure (or depth) at which eruption commenced (Fig. 6b). Thus, if recharge is more important for deep crustal magma chambers, we would expect magmas traversing thicker crust, such as continental crust, to have higher water contents. In this regard, it is noteworthy that Augustine volcano, the most continental of the Aleutian chain volcanoes, has the highest water content along the Aleutian chain (Zimmer and Plank, 2006). REFC also predicts that arc magma water contents would converge to a value defined by the depths at which deep crustal magma chambers form and homogenize, independent of what their original water contents are. It is worth considering the implications of REFC on the two most important differentiation series on Earth, that is, the calc-alkaline and tholeiitic differentiation series. It is generally agreed that high oxygen fugacity and/or water contents drive calc-alkaline differentiation series by triggering magnetite saturation, which in turn leads to Fe depletion and alkali and silica enrichment at relatively constant Mg/(Mg + Fe) (Osborn, 1959; Miyashiro, 1974; Kushiro, 1979; Sisson and Grove, 1993; Zimmer and Plank, 2006). In tholeiitic differentiation series, dry and relatively reduced conditions suppress magnetite crystallization, allowing residual magmas to increase in Fe content. If REFC processes and the depth at which deep crustal magma bodies stage increase with thickness of arc crust, calc-alkaline differentiation series would thus be expected to dominate continental arcs and mature island arcs, whereas tholeiitic series would dominate island arcs and mid-ocean ridges. While there is no doubt that calc-alkaline magmas are almost exclusively found in arc environments, a commonly forgotten observation is that not all arcs are calc-alkaline. As pointed out long ago by Miyashiro (1974), "the main rocks in immature island arcs are usually basalts and basaltic andesites of the tholeiitic series, whereas those in well-developed island arcs with a thick continental-type crust are andesites and dacites of the tholeiitic and calc-alkaline series. The main volcanic rocks in continental margins are andesites, dacites, and rhyolites of the calc-alkaline series." Miyashiro continued further to say that "the proportion of calc-alkaline series rocks among all the volcanic rocks tends to increase with advancing development of continental-type crust beneath the volcanic arc." If these generalizations indeed hold true, it would mean that magmatic processes in the upper crust, like REFC, cannot be ignored when considering the origin of arc magmas. Recently, Chiaradia et al. (2011) showed that incompatible-element enriched basaltic andesites from Ecuador require basaltic recharge in their formation, further suggesting that recharge may be important for generating calc-alkaline differentiation.

In summary, our analysis shows that REFC can generate the elevated H_2O, Fe^{3+}, and CO_2 concentrations in arc magmas without significant decrease in MgO. We emphasize that this *does not* rule out source effects. There is no doubt that the source regions of arc magmas is more water-rich than that of mid-ocean ridge basalts. The purpose of this analysis is to show that REFC can lead to further enrichment of H_2O in arc magmas, resulting in a relatively homogeneous, water-rich parental magma formed in the deep crust. Observed correlations between H_2O/Ce and Nb/Ce have been argued as strong evidence for a source effect (Plank et al., 2013). As discussed above, REFC can fractionate these ratios if their partition coefficients are not identical, but the exact direction of fractionation depends on the relative values of the partition coefficients, which, at this point in time, are not known accurately enough to refute or support REFC control. More work on volatile content of continental arc magmas seems essential to further evaluate REFC.

5.4. Implications for sulfur and chalcophile elements

We can also consider S systematics in a constant mass magma chamber undergoing REFC. If S is in the highest oxidation state, S^{6+}, S will behave as a perfectly incompatible element and will correlate with H_2O, CO_2 and Fe^{3+} enrichments during simultaneous crystallization-recharge. However, if the primary (recharging) magma formed at sulfide saturation in the mantle, as is usually the case (Lee et al., 2012), the dominant oxidation state of S is S^{2-} (Jugo, 2009; Jugo et al., 2010). This initially sulfide-saturated magma will become briefly undersaturated upon ascent into a crustal magma chamber due to the increase in S solubility

Please cite this article in press as: Lee C. -T. A., et al. Modeling the compositional evolution of recharging, evacuating, and fractionating (REFC) magma chambers: Implications for differentiation of arc magmas. *Geochim. Cosmochim. Acta* (2013), http://dx.doi.org/10.1016/j.gca.2013.08.009

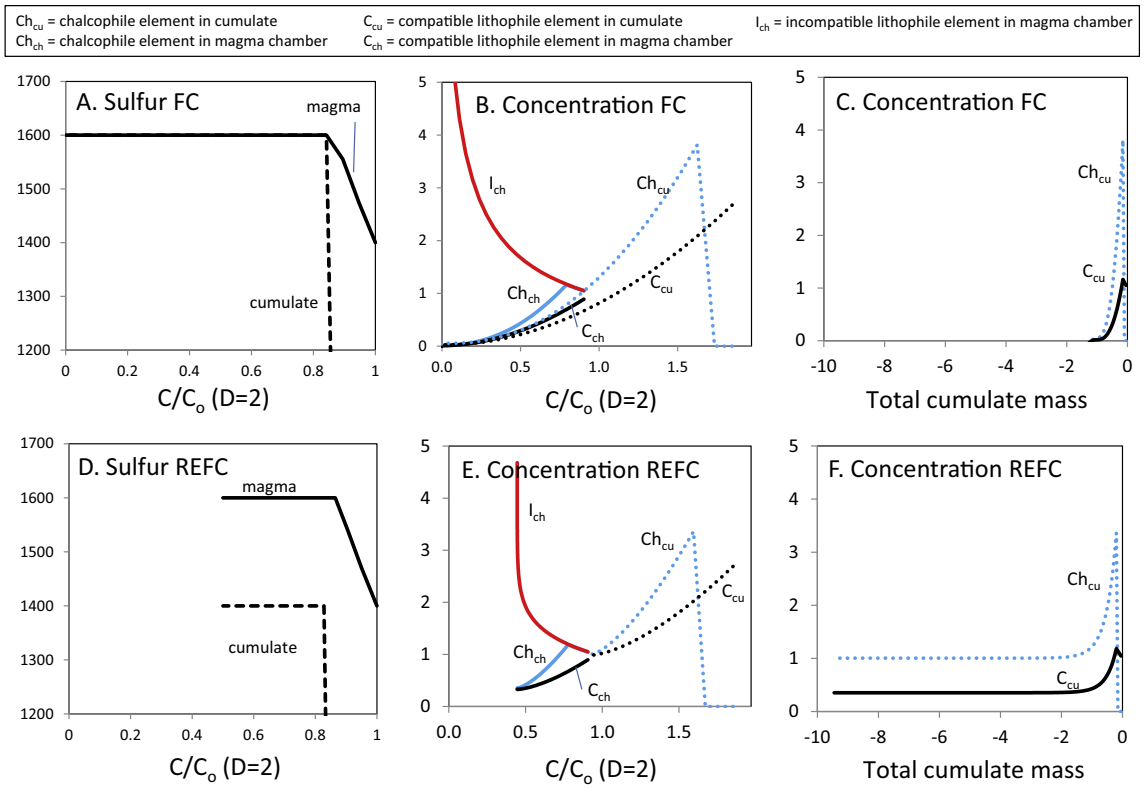

Fig. 7. Behavior of S and chalcophile (*Ch*) elements during (A–C) pure fractional crystallization (FC) and (D–F) during REFC. Behavior of incompatible (*I*) and compatible (*C*) lithophile elements are also shown for reference. (A) S content (ppm) versus relative concentration of an element with compatibility $D = 2$ (similar to Mg) in the magma. Initial S content is 1400 ppm, but the S content at sulfide saturation is assumed to be 1600 ppm so that, initially, the magma is S-undersaturated and S content of the magma rises. Rise of S terminates when saturation at 1600 ppm is achieved. More realistic scenarios where S solubility varies with melt composition are shown in Lee et al. (2012). (B) Relative concentrations of an incompatible lithophile element (I_{ch} with $D = 0.1$), compatible lithophile element (C_{ch}, $D = 3$), and chalcophile element (Ch_{ch}) in the magma chamber plotted versus relative concentration of a compatible lithophile element ($D = 2$) in the magma. Also plotted are the relative concentrations of a chalcophile element (Ch_{cu}) and compatible lithophile element (C_{cu}, $D = 3$) in the cumulate as a function of relative concentration of compatible lithophile element ($D = 2$) in the cumulate. Note rise of I_{ch} and decrease in C_{ch} with progressive fractionational crystallization. Ch_{ch} rises and then decreases as sulfide saturates. (C) Relative concentrations of chalcophile element (Ch_{ch}) and compatible lithophile element (C_{ch}) versus total cumulate mass (values are negative because cumulates treated as subtraction of mass from magma chamber). (D–F) Shows the geochemical behaviors during REFC in a constant mass magma chamber. Symbols as in (A–C). Note that for chalcophile (Ch_{ch}) and *compatible* (C_{ch}) lithophile elements, elemental systematics in the magma during REFC do not differ considerably from pure fractional crystallization, making it difficult to distinguish between the two scenarios (e.g., B and E). (F) Relative concentrations of a chalcophile and compatible lithophile element in the cumulate as a function of total cumulate mass (integrated mass accumulation).

at sulfide saturation with decreasing pressure (O'Neill and Mavrogenes, 2002). S will increase (following Eq. (7a), (7b)) during this interval, but the increase will be brief because the magma will rapidly reach sulfide saturation as the magma cools and evolves (Fig. 7a). After this point, the S content will remain constant at the level of sulfide saturation (Fig. 7). Thus, any further S added by recharging magmas will have to precipitate out of the magma chamber as sulfide-bearing cumulates.

For a constant mass magma chamber, the above scenario can be quantified by setting the left hand side of Eq. (2) to zero so that the S content of the cumulates C_x is given by

$$C_x = (C_{re} - \alpha_e C_e)/\alpha_x \quad (15)$$

For the case in which evacuation and crustal assimilation are zero, the S content of the cumulate must then equal the concentration in the recharging magma. Juvenile basaltic magmas should have ~1200–1600 ppm S, implying similar concentrations in the instantaneous cumulates (Perfit et al., 1983; O'Neill and Mavrogenes, 2002; Liu et al., 2007). For typical magmatic sulfides ((Fe,Ni)S), this corresponds to ~0.33–0.39 wt.% sulfide mode in the cumulate fraction. By contrast, the S content of fertile mantle is ~200 ppm, corresponding to ~0.06% sulfide (Lorand, 1989, 1990). These differences in sulfide mode will have profound effects on the behavior of sulfide-loving elements (chalcophile elements), such as Cu (Lee et al., 2012). For example, the partitioning of Cu between sulfide and silicate melt is ~800 (Lynton et al., 1993; Gaetani and Grove, 1997;

Ripley et al., 2002), so the bulk D for Cu would be ~0.4 during peridotite melting and ~2.6 during crystallization from a magma, resulting in a fundamental switch from incompatible during mantle melting to compatible during crystallization from a magma chamber (Lee et al., 2012). This difference in sulfide mode corresponds to a factor of 6–7 increase in the bulk solid/melt partition coefficient of a highly chalcophile (sulfide-loving) element during crystallization compared to melting of the mantle.

Fig. 7 shows that the behavior of a chalcophile element (e.g., Cu) relative to a compatible lithophile element (e.g., MgO) during magma differentiation for pure fractional crystallization and REFC are actually similar, making it difficult to distinguish between these processes (Fig. 7b and e). The main difference, however, is that magmas undergoing REFC will have generated larger amounts of sulfide-bearing and chalcophile element-rich cumulates (Fig. 7f).

For growing or dying magma chambers, the situation is more complex. Dying magma chambers, where magma chamber mass is decreasing, will result in rapid approach to saturation if S is in the reduced state. Growing magma chambers have the capacity to suppress sulfide fractionation due to the diluting effects of recharge by S-undersaturated magmas. These problems can be dealt with using the more general equations in the Appendix.

5.5. Implications for coupled effects of Fe and S redox

A final issue worth exploring is the redox reactions between Fe and S species during REFC. We can consider the case in which the primary magma begins with an Fe^{3+}/Fe_T of 0.1 and a S^{2-}/S_T of 1, that is, the Fe oxidation state is mixed and the S oxidation state is all in the 2- state. As discussed above, in a system whose oxygen fugacity is not buffered, REFC will cause Fe^{3+} to increase, but some of this increase would be consumed by reacting with S^{2-}, causing oxidation of S^{2-} to S^{6+} and reduction of Fe^{3+} back to Fe^{2+}. Eight electrons are required to oxidize S^{2-} to S^{6+} while one electron is required to reduce Fe^{3+} to Fe^{2+}, that is,

$$8Fe^{2+} + S^{6+} = 8Fe^{3+} + S^{2-} \quad (16)$$

A typical primitive basalt has 8–9 wt.% FeO and ~2000 ppm S if it originated by sulfide-saturated melting in the mantle. This corresponds to 0.11–0.13 moles of Fe and 0.006 moles of S per 100 g of magma, translating to a molar Fe/S ratio of 17–20, which is significantly higher than the stoichiometric Fe/S ratio of 8 in the above reaction. This implies that, in general, the oxidation state of S will follow the oxidation state of Fe during basalt differentiation, raising the interesting possibility that recharge-crystallization will cause correlated increases in H_2O, CO_2, Fe^{3+}/Fe_T as well as S^{6+}/S_T with little or no correlation with compatible elements, such as Mg, which are traditionally used as indices of differentiation.

5.6. Caveats and limitations

There are obvious caveats to the entire analysis of REFC presented here. The first is that we have not considered an energy balance and have thus ignored latent heat (Bohrson and Spera, 2001). While this is beyond the scope of our manuscript, the reader should use geologic and thermodynamic common sense when exploring the above equations. We clearly have not considered fluid dynamics and non-equilibrium conditions. Our models are box models, so we have assumed that any assimilant or recharging magma is instantaneously homogenized in the magma chamber. Homogenization is unlikely to be efficient in felsic systems due to the very high viscosities of such magmas, so the equations used above are probably only applicable to hot magmas, such as basaltic systems. The issue of crystal mushes is also not considered as we have assumed that what erupts is a liquid and representative of the magma chamber minus the crystals. We also do not consider phase equilibria directly because this is difficult to implement in analytical solutions. Nevertheless, in the attached software (Appendix), the reader can roughly simulate changes in the crystallizing phase assemblage by allowing bulk D to change. In reality, a more accurate model of crystallizing phase assemblage will inevitably require coupling these mass balance equations with thermodynamically constrained phase equilibria using programs, such as MELTS (Asimow and Ghiorso, 1998; Ghiorso et al., 2002). The analytical and semi-analytical approaches presented here nevertheless provide a simple, accessible and intuitive way of understanding the behavior of REFC and REAFC systems. Finally, we have not considered the effects of changing the composition of recharging magma with time because this is difficult to implement analytically. However, this is trivial to implement using numerical approaches presented in Appendix A3.

6. CONCLUSIONS

Analytical equations describing recharging, evacuating, and fractionally crystallizing (REFC) magma chambers are presented here with additional equations for assimilation (REAFC) shown in the Appendix. We show that simultaneous recharge and crystallization can explain many of the geochemical signatures of arc magmas, such as enrichments in volatiles and other incompatible elements. These equations are general enough to account for growing or dying magma bodies as well as steady-state magma chambers and are thus applicable to melt-rock reaction processes, wherein a magma rising through a dike reacts with the wallrock, resulting in dissolution and/or crystal precipitation (Kelemen, 1990a,b; Kelemen et al., 1998).

In summary, we propose that arc magmas may go through multi-stage histories, beginning with the generation of primary hydrous mantle-derived magmas from the mantle wedge. These magmas then rise into the lower crust, where they stage in long-lived magma chambers, are subjected to continuous recharge and fractional crystallization, generating a second stage magma from which all subsequent derivative liquids originate. Incompatible elements will become enriched in this second stage magma but compatible elements will be only slightly depleted. Crustal magmas will therefore inherit their compositions from this deep crustal recharging zone. Estimating primary, mantle-derived magma compositions from these second

Please cite this article in press as: Lee C. -T. A., et al. Modeling the compositional evolution of recharging, evacuating, and fractionating (REFC) magma chambers: Implications for differentiation of arc magmas. *Geochim. Cosmochim. Acta* (2013), http://dx.doi.org/10.1016/j.gca.2013.08.009

stage magmas will thus over-estimate the incompatible element concentration of the mantle source.

ACKNOWLEDGMENTS

We thank Francis Albarede, Emily Chin, Rajdeep Dasgupta, Monica Erdman, Michael Farner, Charlie Langmuir, Hugh O'Neill, Peter Luffi, Anukriti Sharma, Xu-Jie Shu, Claudia Sayao Valladares, and Qing-zhu Yin for discussions. This research was supported by NSF OCE-1338842. We thank Jeremy Richards and two anonymous reviewers for constructive and helpful comments.

APPENDIX A

A.1. Recharge, evacuation, assimilation and fractional crystallization in magma chamber at steady state mass (REAFC)

Eqs. (7a) and (7b) can be generalized to include crustal assimilation, yielding an equation that accounts for continuous simultaneous recharge, evacuation/eruption, assimilation and fractional crystallization (REAFC). If the magma chamber mass is constant, the following mass balance holds:

$$dM_x + dM_e = dM_{re} + dM_{cc} \tag{A1}$$

where dM_{cc} is the mass added to the magma chamber by crustal assimilation and all other symbols as described in the main text. Elemental mass balance is then given by

$$M_{ch}dC_{ch} = (-D\alpha_x C_{ch} - \alpha_e C_{ch} + C_{cc}\alpha_{cc} + C_{re})dM_{re} \tag{A2}$$

where C_{cc} is the concentration in the crustal wallrock, $\alpha_{cc} \equiv dM_{cc}/dM_{re}$, and all other symbols as described previously. Integrating, yields a more general form of Eqs. (7a) and (7b)

$$C_{ch} = \frac{C_{re} + C_{cc}\alpha_{cc}}{D\alpha_x + \alpha_e} - \left[\frac{C_{re} + C_{cc}\alpha_{cc}}{D\alpha_x + \alpha_e} - C^o_{ch}\right] \exp\left[-\Delta\overline{M}_{re}(D\alpha_x + \alpha_e)\right] \tag{A3}$$

This equation can be simplified if the composition of the recharging magma is the same as the original magma composition

$$\frac{C_{ch}}{C^o_{ch}} = \frac{1 + \alpha_{cc}C_{cc}/C^o_{ch}}{D\alpha_x + \alpha_e} - \left[\frac{1 + \alpha_{cc}C_{cc}/C^o_{ch}}{D\alpha_x + \alpha_e} - 1\right] \exp\left[-\Delta\overline{M}_{re}(D\alpha_x + \alpha_e)\right] \tag{A4}$$

A.2. REAFC for growing and dying magma chambers

This section presents the general case of a non-steady state magma chamber undergoing recharge, evacuation/eruption, assimilation, and fractional crystallization. The change in mass of a magma chamber is given by

$$dM_{ch} = dM_x + dM_e + dM_{re} + dM_{cc} \tag{A5}$$

where dM_x, dM_e, dM_{re}, and dM_{cc} are the change in total mass of the magma chamber due to crystallization, evacuation, recharge and crustal assimilation. Here, dM_i is <0 if mass is being *removed* from the magma chamber and >0 if mass is being *added*. Thus, dM_x and dM_e are always negative, dM_{re} and dM_{cc} are always positive, and dM_{ch} is positive if the magma chamber is growing or negative if it is decreasing. Mass balance for a given element is then given by

$$dm_{ch} = C_x dM_x + C_{ch}dM_e + C_{re}dM_{re} + C_{cc}dM_{cc} \tag{A6}$$

where dm_{ch} is the change in mass of a given element in the magma chamber. We then define fractional quantities relating the ratio of mass added/subtracted associated with a given process to the change in mass of the magma chamber

$$\begin{aligned}\phi_x &= dM_x/dM_{ch}\\ \phi_e &= dM_e/dM_{ch}\\ \phi_{re} &= dM_{re}/dM_{ch}\\ \phi_{cc} &= dM_{cc}/dM_{ch}\end{aligned} \tag{A7}$$

The sign of these fractional quantities will depend on whether the magma chamber mass is increasing or decreasing. For example, ϕ_x is < 0 when the magma chamber mass is decreasing ($dM_{ch} < 0$) and is >0 when the magma chamber mass is increasing ($dM_{ch} > 0$). Eq. (A6) can be re-expressed as follows by substituting in Eq. (A7) and the partition coefficient D:

$$dm_{ch} = \left(\frac{Dm_{ch}\phi_x}{M_{ch}} + \frac{m_{ch}\phi_e}{M_{ch}} + C_{re}\phi_{re} + C_{cc}\phi_{cc}\right)dM_{ch} \tag{A8}$$

Eq. (A8) is a linear first-order differential equation that can be integrated using an integration factor. This leads to

$$C_{ch} = C^o_{ch}F^{D\phi_x+\phi_e-1} + \frac{C_{re}\phi_{re} + C_{cc}\phi_{cc}}{D\phi_x + \phi_e - 1}\left[F^{D\phi_x+\phi_e-1} - 1\right] \tag{A9}$$

where F is the ratio of the magma chamber mass relative to the initial magma chamber mass

$$F = M_{ch}/M^o_{ch} \tag{A10}$$

and is <1 if the magma chamber mass is decreasing and >1 if increasing. The composition of the cumulate at any instant is obtained by multiplying C_{ch} by the bulk solid/liquid partition coefficient D. Note that if recharge, evacuation and crustal assimilation are zero ($\phi_{re} = \phi_e = \phi_{cc} = 0$ and $\phi_x = 1$), it can be seen that Eq. (A9) simplifies to the Rayleigh fraction equation (Eq. (1a)), where F is the residual liquid fraction after crystal segregation. If evacuation and recharge are zero, then the above equation is the same as DePaolo's (1981) equations for assimilation and fractional crystallization (e.g., AFC process). We can also consider the unrealistic end-member case in which crystallization and evacuation are zero ($\phi_x = \phi_e = 0$). Under these conditions, the magma chamber will grow indefinitely and we would expect the composition of this growing magma chamber to eventually converge to a weighted average between the recharging magma and crustal assimilant. As expected, when F is $\gg 1$, we find that $C_{ch} \sim C_{re}\phi_{re} + C_{cc}\phi_{cc}$.

Please cite this article in press as: Lee C. -T. A., et al. Modeling the compositional evolution of recharging, evacuating, and fractionating (REFC) magma chambers: Implications for differentiation of arc magmas. *Geochim. Cosmochim. Acta* (2013), http://dx.doi.org/10.1016/j.gca.2013.08.009

A.3. Excel program for REAFC

A Microsoft Excel spreadsheet is provided to support the above equations. One worksheet called "REFC-analytical-constantmass" is for REFC processes in a constant mass magma chamber and uses the analytical solutions shown above. D is assumed to be constant. For the more general case of a growing/dying magma chamber undergoing REFC, the reader should use the "REFC-analytical-changingmass" worksheet. D is assumed to be constant here as well. In case a variable D is desired, a numerical approach is required. This is given in the worksheet "REAFC-generalnumerical", which also accounts for crustal assimilation.

APPENDIX B. SUPPLEMENTARY DATA

Supplementary data associated with this article can be found, in the online version, at http://dx.doi.org/10.1016/j.gca.2013.08.009.

REFERENCES

Albarede F. (1985) Regime and trace-element evolution of open magma chambers. *Nature* **318**, 356–358.

Albarede F. (1996) *Introduction to Geochemical Modeling*. Cambridge University Press.

Annen C., Blundy J. D. and Sparks R. S. J. (2006) The genesis of intermediate and silicic magmas in deep crustal hot zones. *J. Petrol.* **47**, 505–539.

Asimow P. D. and Ghiorso M. S. (1998) Algorithmic modifications extending MELTS to calculate subsolidus phase relations. *Am. Mineral.* **83**, 1127–1132.

Bohrson W. A. and Spera F. J. (2001) Energy-constrained open-system magmatic processes II: Application of energy–constrained assimilation fractional crystallization (EC–AFC) model to magmatic systems. *J. Petrol.* **42**, 1019–1041.

Canil D., O'Neill H. S. C., Pearson D. G., Rudnick R. L., McDonough W. F. and Carswell D. A. (1994) Ferric iron in peridotites and mantle oxidation states. *Earth Planet. Sci. Lett.* **123**, 205–220.

Carmichael I. S. E. (1991) The redox states of basic and silicic magmas: A reflection of their source regions? *Contrib. Mineral. Petrol.* **106**, 129–141.

Chaussard E. and Amelung F. (2012) Precurosry inflation of shallow magma reservoirs at west Sunda volcanoes detected by InSAR. *Geophys. Res. Lett.* **39**.

Chiaradia M., Müntener O. and Beate B. (2011) Enriched basaltic andesites from mid-crustal fractional crystallization, recharge, and assimilation (Pilavo Volcano, Western Cordillera of Ecuador). *J. Petrol.* **52**, 1107–1141.

Collier M. L. and Kelemen P. B. (2010) The case for reactive crystallization at mid-ocean ridges. *J. Petrol.* **51**, 1913–1940.

DeBari S. M. and Sleep N. H. (1991) High-Mg, low-Al bulk composition of the Talkeetna island arc, Alaska: Implications for primary magmas and the nature of arc crust. *Geol. Soc. Am. Bull.* **103**, 37–47.

DePaolo D. J. (1981) Trace element and isotopic effect of combined wallrock assimilation and fractional crystallization. *Earth Planet. Sci. Lett.* **53**, 189–202.

Ducea M. N. (2002) Constraints on the bulk composition and root foundering rates of continental arcs: A California arc perspective. *J. Geophys. Res.* **107**. http://dx.doi.org/10.1029/2001JB000643.

Ducea M. N. and Saleeby J. B. (1996) Buoyancy sources for a large, unrooted mountain range, the Sierra Nevada, California: Evidence from xenolith thermobarometry. *J. Geophys. Res.* **101**, 8229–8244.

Ducea M. N. and Saleeby J. B. (1998) The age and origin of a thick mafic-ultramafic keel from beneath the Sierra Nevada batholith. *Contrib. Mineral. Petrol.* **133**, 169–185.

Dufek J. and Bergantz G. W. (2005) Lower crustal magma genesis and preservation: A stochastic framework for the evaluation of basalt-crust interaction. *J. Petrol.* **46**, 2167–2195.

Gaetani G. A. and Grove T. L. (1997) Partitioning of moderately siderophile elements among olivine, silicate melt, and sulfide melt: Constraints on core formation in the Earth and Mars. *Geochim. Cosmochim. Acta* **61**, 1829–1846.

Gast P. W. (1968) Trace element fractionation and the origin of tholeiitic and alkaline magma types. *Geochim. Cosmochim. Acta* **32**, 1057–1086.

Gelman S. E., Gutierrez F. J. and Bachmann O. (2013) On the longevity of large upper crustal silicic magma reservoirs. *Geology*. http://dx.doi.org/10.1130/G34241.1.

Ghiorso M. S., Hirschmann M. M., Reiners P. W. and Kress V. C. (2002) The pMELTS: A revision of MELTS for improved calculation of phase relations and major element partitioning related to partial melting of the mantle to 3 GPa. *Geochem. Geophys. Geosys.* **3**. http://dx.doi.org/10.1029/2001GC000217.

Gill J. B. (1981) *Orogenic Andesites and Plate Tectonics*. Springer, Berlin.

Greenland L. P. (1970) An equation for trace element distribution during magmatic crystallization. *Am. Mineral.* **55**, 455–465.

Herzberg C. and Asimow P. D. (2008) Petrology of some oceanic island basalts: PRIMELT2.XLS software for primary magma calculation. *Geochem. Geophys. Geosys.* **9**. http://dx.doi.org/10.1029/2008GC002057.

Herzberg C., Asimow P. D., Arndt N. T., Niu Y., Lesher C. M., Fitton J. G., Cheadle M. J. and Saunders A. D. (2007) Temperatures in ambient mantle and plumes: Constraints from basalts, picrites and komatiites. *Geochem. Geophys. Geosys.* **8**. http://dx.doi.org/10.1029/2006GC001390.

Hill R. I. (1988) San Jacinton intrusive complex 1. Geology and mineral chemistry, and a model for intermittent recharge of tonalitic magma chambers. *J. Geophys. Res.* **93**, 10325–10348.

Hill R. I., Silver L. T., Taylor, Jr., H. P. and Chappell B. W. (1985) Solidification and recharge of SiO_2-rich plutonic magma chambers. *Nature* **313**, 643–646.

Hofmann A. W. (2012) Magma chambers on a slow burner. *Nature* **49**, 677–678.

Jagoutz O. E. (2010) Construction of the granitoid crust of an island arc. Part II: A quantitative petrogenetic model. *Contrib. Mineral. Petrol.* **160**, 359–381.

Jagoutz O., Muntener O., Ulmer P., Pettke T., Burg J.-P., Dawood H. and Hussain S. (2007) Petrology and mineral chemistry of lower crustal intrusions: The Chilas Complex Kohistan (NW Pakistan). *J. Petrol.* **48**, 1895–1953.

Jellinek A. M. and DePaolo D. J. (2003) A model for the origin of large silicic magma chambers: Precursors of caldera-forming eruptions. *Bull. Volcanol.* **65**, 363–381.

Jicha B. R., Scholl D. W., Singer B. S., Yogodzinski G. M. and Kay S. M. (2006) Revised age of Aleutian island arc formation implies high rate of magma production. *Geology* **34**, 661–664.

Jugo P. J. (2009) Sulfur content at sulfide saturation in oxidized magmas. *Geology*, 415–418.

Jugo P. J., Wilke M. and Botcharnikov R. E. (2010) Sulfur K-edge XANES analysis of natural and synthetic basaltic glasses: Implications for S speciation and S content as function of oxygen fugacity. *Geochim. Cosmochim. Acta* **74**, 5926–5938.

Please cite this article in press as: Lee C. -T. A., et al. Modeling the compositional evolution of recharging, evacuating, and fractionating (REFC) magma chambers: Implications for differentiation of arc magmas. *Geochim. Cosmochim. Acta* (2013), http://dx.doi.org/10.1016/j.gca.2013.08.009

Karlstrom L., Dufek J. and Manga M. (2010) Magma chamber stability in arc and continental crust. *J. Volcanol. Geotherm. Res.* **190**, 249–270.

Kelemen P. B. (1990a) Reaction between ultramafic rock and fractionating basaltic magma I. Phase relations, the origin of calc-alkaline magma series, and the formation of discordant dunite. *J. Petrol.* **31**, 51–98.

Kelemen P. B. (1990b) Reaction between ultramafic rock and fractionating basaltic magma II. Experimental investigation of reaction between olivine tholeiite and harzburgite at 1150–1050 °C and 5 kb. *J. Petrol.* **31**, 99–134.

Kelemen P. B., Hart S. R. and Bernstein S. (1998) Silica enrichment in the continental upper mantle via melt/rock reaction. *Earth Planet. Sci. Lett.* **164**, 387–406.

Kelley K. A. and Cottrell E. (2009) Water and the oxidation state of subduction zone magmas. *Science* **325**, 605–607.

Kushiro I. (1979) Fractional crystallization of basaltic magma. In *The Evolution of the Igneous Rocks: Fiftieth Anniversary Perspectives* (ed. H. S. Yoder). Princeton University Press, Princeton, pp. 171–203.

Lasaga A. C. (1998) *Kinetic Theory in the Earth Sciences*. Princeton University Press, Princeton.

Lee C.-T. A. (2013) Physics and chemistry of deep continental crust recycling. *Treatise of Geochemistry*, in press.

Lee C.-T. A., Cheng X. and Horodyskyj U. (2006) The development and refinement of continental arcs by primary basaltic magmatism, garnet pyroxenite accumulation, basaltic recharge and delamination: Insights from the Sierra Nevada, California. *Contrib. Mineral. Petrol.*. http://dx.doi.org/10.1007/s00410-00005-00056-00411.

Lee C.-T. A., Morton D. M., Kistler R. W. and Baird A. K. (2007) Petrology and tectonics of Phanerozoic continent formation: From island arcs to accretion and continental arc magmatism. *Earth Planet. Sci. Lett.* **263**, 370–387.

Lee C.-T. A., Luffi P., Plank T., Dalton H. A. and Leeman W. P. (2009) Constraints on the depths and temperatures of basaltic magma generation on Earth and other terrestrial planets using new thermobarometers for mafic magmas. *Earth Planet. Sci. Lett.* **279**, 20–33.

Lee C.-T. A., Luffi P., Chin E. J., Bouchet R., Dasgupta R., Morton D. M., Le Roux V., Yin Q.-Z. and Jin D. (2012) Copper systematics in arc magmas and implications for crust-mantle differentiation. *Science* **336**, 64–68.

Leeman W. P. (1996) Boron and other fluid-mobile elements in volcanic arc lavas: Implications for subduction processes. In *Subduction Top to Bottom* (eds. G. E. Bebout, D. Scholl, S. Kirby and J. P. Platt). AGU Monograph, pp. 269–276.

Liu Y., Samaha N.-T. and Baker D. R. (2007) Sulfur concentration at sulfide saturation (SCSS) in magmatic silicate melts. *Geochem. Cosmochim. Acta* **71**, 1783–1799.

Lorand J.-P. (1989) Abundance and distribution of Cu–Fe–Ni sulfides, sulfur, copper and platinum-group elements in orogenic-type spinel lherzolite massifs of Ariège (northeastern Pyrenees, France). *Earth Planet. Sci. Lett.* **93**, 50–64.

Lorand J. P. (1990) Are spinel lherzolite xenoliths representative of the abundances of sulfur in the upper mantle? *Geochim. Cosmochim. Acta* **54**, 1487–1492.

Lynton S. J., Candela P. A. and Piccoli P. M. (1993) An experimental study of the partitioning of copper between pyrrhotite and a high silica rhyolitic melt. *Econ. Geol.* **88**, 901–915.

Miyashiro A. (1974) Volcanic rock series in island arcs and active continental margins. *Am. J. Sci.* **274**, 321–355.

Mukhopadhyay B. and Manton W. I. (1994) Upper mantle fragments from beneath the Sierra Nevada batholith-partial fusion, fractional crystallization and metasomatism in subduction-related ancient lithosphere. *J. Petrol.* **35**, 1418–1450.

Norton D. L. (1984) Theory of hydrothermal systems. *Annu. Rev. Earth Planet. Sci.* **12**, 155–177.

O'Hara M. J. (1977) Geochemical evolution during fractional crystallization of a periodically refilled magma chamber. *Nature* **266**, 503–507.

O'Hara M. J. and Matthews R. E. (1981) Geochemical evolution in an advancing, periodically replenished, periodically tapped, continuously fractionated magma chamber. *J. Geol. Soc.* **138**, 237–277.

O'Neill H. S. C. and Mavrogenes J. A. (2002) The sulfide capacity and the sulfur content at sulfide saturation of silicate melts at 1400 °C and 1 bar. *J. Petrol.* **43**, 1049–1087.

O'Neill H. S. C. and Jenner F. (2012) The global pattern of trace-element distributions in ocean floor basalts. *Nature* **491**, 698–705.

Osborn E. F. (1959) Role of oxygen partial pressure in the crystallization and differentiation of basaltic magma. *Am. J. Sci.* **257**, 609–647.

Perfit M. R., Fornari D. J., Malahoff A. and Embley R. W. (1983) Geochemical studies of abyssal lavas recovered by DSRV Alvin from eastern Galapagos Rift, Inca Transform, and Ecuador Rift 3. Trace element abundances and petrogenesis. *J. Geophys. Res.* **88**, 10551–10572.

Plank T., Kelley K. A., Zimmer M. M., Hauri E. H. and Wallace P. J. (2013) Why do mafic arc magmas contain ~4 wt% water on average? *Earth Planet. Sci. Lett.* **364**, 168–179.

Putirka K. D. (2005) Mantle potential temperatures at Hawaii, Iceland, and the mid-ocean ridge system, as inferred from olivine phenocrysts: Evidence for thermally driven mantle plumes. *Geochem. Geophys. Geosys.* **6**. http://dx.doi.org/10.1029/2005GC000915.

Putirka K. D., Perfit M., Ryerson F. J. and Jackson M. G. (2007) Ambient and excess mantle temperatures, olivine thermometry, and active vs. passive upwelling. *Chem. Geol.* **241**, 177–206.

Ripley E. M., Brophy J. G. and Li C. (2002) Copper solubility in a basaltic melt and sulfide liquid/silicate melt partition coefficients of Cu and Fe. *Geochim. Cosmochim. Acta* **66**, 2791–2800.

Rubin A. M. (1995) Propagation of magma-filled cracks. *Annu. Rev. Earth Planet. Sci.* **23**, 287–336.

Shaw D. M. (1970) Trace element fractionation during anatexis. *Geochim. Cosmochim. Acta* **34**, 237–243.

Shaw D. M. (1979) Trace element melting models. *Phys. Chem. Earth* **11**, 577–586.

Sisson T. W. and Grove T. L. (1993) Experimental investigations of the role of H_2O in calc-alkaline differentiation and subduction zone magmatism. *Contrib. Mineral. Petrol.* **113**, 143–166.

Till C. B., Grove T. L. and Krawczynski M. J. (2012) A melting model for variably depleted and enriched lherzolite in the plagioclase and spinel stability fields. *J. Geophys. Res.* **117**. http://dx.doi.org/10.1029/2011JB009044.

Uyeda S. (1982) Subduction zones: An introduction to comparative subductology. *Tectonophys* **81**, 133–159.

Uyeda S. and Kanamori H. (1979) Back-arc opening and the mode of subduction. *J. Geophys. Res.* **84**, 1049–1061.

Weaver J. S. and Langmuir C. H. (1990) Calculation of phase equilibrium in mineral-melt systems. *Comput. Geosci.* **16**, 1–19.

Witham F., Blundy J., Kohn S., Lesne P., Dixon J. E., Churakov S. V. and Botcharnikov R. E. (2012) SolEx: A model for mixed COHSCl-volatile solubilities and exsolved gas compositions in basalt. *Comput. Geosci.* **45**, 87–97.

Zimmer M. M. and Plank T. (2006) The role of water in generating Fe-depletion and the calc-alkaline trend. *EOS Trans. AGU* **87**(52), V23C-0636.

Zou H. (2007) *Quantitative Geochemistry*. Imperical College Press, London.

Associate editor: Weidong Sun